Pacific Northwest
NATIONAL LABORATORY

PNNL-33005

Capability to Process and Characterize Uranium-Zirconium (U-Zr) and Uranium-Zirconium-Plutonium (U-Zr-Pu) Alloys

June 2022

MT Athon
M McCoy,
CA Lavender
PJ MacFarlan,
DD Reilly
A Devaraj
LE Sweet
Huber, Zachary

U.S. DEPARTMENT OF ENERGY

Prepared for the U.S. Department of Energy
under Contract DE-AC05-76RL01830

DISCLAIMER

PACIFIC NORTHWEST NATIONAL LABORATORY
operated by
BATTELLE
for the
UNITED STATES DEPARTMENT OF ENERGY
under Contract DE-AC05-76RL01830

Printed in the United States of America

Available to DOE and DOE contractors from the Office of Scientific and Technical Information,
P.O. Box 62, Oak Ridge, TN 37831-0062
www.osti.gov
ph: (865) 576-8401
fax: (865) 576-5728
email: reports@osti.gov

Available to the public from the National Technical Information Service
5301 Shawnee Rd., Alexandria, VA 22312
ph: (800) 553-NTIS (6847)
or (703) 605-6000
email: info@ntis.gov
Online ordering: http://www.ntis.gov

PNNL-33005

Capability to Process and Characterize Uranium-Zirconium (U-Zr) and Uranium-Zirconium-Plutonium (U-Zr-Pu) Alloys

June 2022

MT Athon
M McCoy,
CA Lavender
PJ MacFarlan,
DD Reilly
A Devaraj
LE Sweet
ZF Huber

Prepared for
the U.S. Department of Energy
under Contract DE-AC05-76RL01830

Pacific Northwest National Laboratory
Richland, Washington 99354

Summary

This work investigated co-reduction of anhydrous compounds of uranium, zirconium, and plutonium to produce uranium rich ternary nuclear fuel alloys. Metallothermic co-reduction is a novel method to produce all-metal nuclear fuels. Metal fuels offer thermal, fissility, compatibility, and security benefits over oxide fuels. Alloys of uranium–10% zirconium with plutonium contents of 0%, 2.5%, 5%, and 10% were produced, with yields of 60–85% of theoretical values in a traditional calciothermic bomb reduction apparatus. Microstructural analysis indicated transformation of uranium phase from gamma to beta and then alpha, in alternating lamellar plates typical of alpha phase uranium and delta phase uranium-zirconium, with zirconium and carbides at prior grain boundaries. Some of the analyses were inconclusive in their results and therefore require additional testing. Successful ternary co-reduction would simplify production of homogeneous feedstock and thereby streamline manufacture of homogeneous ternary metallic fuel.

Acknowledgments

This research was supported by the Energy and Environment Directorate (EED) Mission Seed, under the Laboratory Directed Research and Development (LDRD) Program at Pacific Northwest National Laboratory (PNNL). PNNL is a multiprogram national laboratory operated for the U.S. Department of Energy (DOE) by Battelle Memorial Institute under Contract No. DE-AC05-76RL01830.

Acronyms and Abbreviations

APT	atom probe tomography
DOE	U.S. Department of Energy
EDS	energy dispersive spectroscopy
FIB	focused ion beam
FFTF	Fast Flux Test Facility
PNNL	Pacific Northwest National Laboratory
SEM	scanning electron microscopy
SS	stainless steel
TEM	transmission electron microscopy
U-Zr-Pu	uranium-zirconium-plutonium
U-10Zr-Pu	uranium 10 weight % zirconium-plutonium
VIM	vacuum induction melting
XRD	x-ray diffraction

Contents

Figures

1.0 Introduction

This work is focused on the co-reduction of anhydrous compounds of uranium (U), zirconium (Zr), and plutonium (Pu) to produce U-rich ternary nuclear fuel alloys. This is a novel method to produce metallic nuclear fuels. Uranium-zirconium (U-Zr) metal alloys with and without plutonium have been used in nuclear reactors such as the Experimental Breeder Reactors I and II (EBR-I and EBR-II) and the Fast Flux Test Facility (FFTF) (C.B. Basak, Prabhu, and Krishnan 2010; Carmack et al. 2009; Hofman, Walters, and Bauer 1997; Zhang et al. 2016). Metallic fuels provide many benefits over ceramic fuels including higher thermal conductivity and higher fissile material density. Additionally, metal fuels are compatible with austenitic stainless steel (SS) cladding and corrosive coolants such as sodium (C.B. Basak, Prabhu, and Krishnan 2010; Carmack et al. 2009; Hofman, Walters, and Bauer 1997; Zhang et al. 2016). When irradiated, plutonium alloy fuels have been shown to increase fuel/cladding interactions that arise from the solubility of plutonium in iron (Nakamura et al. 2012).

Substitution of plutonium for U-235 enrichment within a fuel has been proposed as a use for excess plutonium. Furthermore, because pyroprocessing as a metal recovery method has a low uranium/plutonium separation efficiency, it is viewed as reducing proliferation concern. However, the fabrication of U-Zr-Pu metal fuels has its own challenges.

High purity, phase consistent U-Zr-Pu feedstock can be a challenge to produce because molten zirconium is a reducing agent. High levels of carbon (>500 ppm) and inclusions with very low actinide solubility (<1%) such as carbon, oxygen, and/or nitrogen-stabilized, alpha-phase Zr are common issues with U-Zr-Pu fabrication. Typically, vacuum induction melting (VIM) is used to produce actinide alloys on a kilogram scale. Graphite crucibles and molds are commonly used in VIM systems. However, producing a homogeneous alloy can be difficult in the graphite crucible of a VIM system, because induction mixing with a graphite inductor can be insufficient. Furthermore, thermomechanical processes often subject as-cast alloys to multiphase temperature profiles that promote multiphase microstructural regions (McCoy et al. 2020). The metallothermic reduction process is likely to overcome this challenge by its use of intimately mixed, micron-sized U, Zr, and Pu powders that are rapidly reduced to a bulk metal form.

Historically, co-reduction has been applied for binary alloy formation. The method applied here uses U and Zr fluorides with Pu oxide. The use of Pu oxide eliminates the difficulties that accompany the development of Pu fluorides. However, as stated above, a major challenge with the production of Zr alloys lies in the creation of an oxygen- and/or nitrogen-stabilized form of the alpha Zr phase. This phase has very low solubility for actinides, which would typically discourage the use of an oxide in production methods. However, in this application, the metallothermic reductant, calcium (Ca), has a greater affinity for oxygen than Zr has. Also, the Pu oxide is limited to a concentration typical of Pu metal content in fast nuclear reactor fuel. The high-surface-area interactions among U, Zr, and Pu in compounds in the co-reduction process, as compared to more traditional metal casting methods, increases the availability of Zr for actinide diffusion.

With these alloys, actinide diffusion into Zr must occur before the oxygen/nitrogen-stabilized phase forms, because this phase behaves as a diffusion barrier. Ultimately, the ternary co-reduction method simplifies the production of a homogeneous feedstock, which helps streamline the process for manufacture of a homogeneous alloy.

To explore the microstructure of the U-Zr-Pu ternary system produced via metallothermic reduction, PNNL produced four ~10 g “buttons” of uranium-10wt%-zirconium-plutonium (U-10Zr-Pu) alloys with nominal weight fractions of 0%, 2.5%, 5%, and 10%Pu. These buttons were sectioned and analyzed for microstructural features and impurity content with scanning electron microscopy–energy-dispersive x-ray spectroscopy (SEM-EDS), transmission electron microscopy (TEM), focused ion beam (FIB), and atom probe tomography (APT).

2.0 Materials and Methods

The reduction of UF_4 to U metal has been the primary production method for uranium metal since the 1940s. The process is commonly known as either the Ames process, because it was developed for U production at Ames Laboratory during the Manhattan Project; the Baker process, after the Los Alamos plutonium scientist R.D. Baker; or the bomb reduction process, because it is typically conducted within a calorimeter-type bomb vessel Historically, the process was known to have “blowouts” from the pressurization of iodine vapor used to enhance the energy of the reaction. Therefore, the process as conducted for this research used a modified reduction vessel that prevented pressurization. This in turn required the vessel to be housed within an argon filled chamber to prevent the influx of oxygen during operation.

Furthermore, the vessel was required to have high-temperature corrosion resistance for the exposure to iodine, fluorine, and other chemical vapors as well as some mechanical strength at +1400°C. Tantalum and 309 SS satisfied these requirements. Magnesium oxide crucibles fit within the vessels to prevent interaction between the vessel walls and molten metal. The maximum volume of each crucible was 20 ml. The crucibles were additively manufactured and sintered at 1650°C. Figure 1 and Figure 2 illustrate the vessel and crucible designs, respectively.

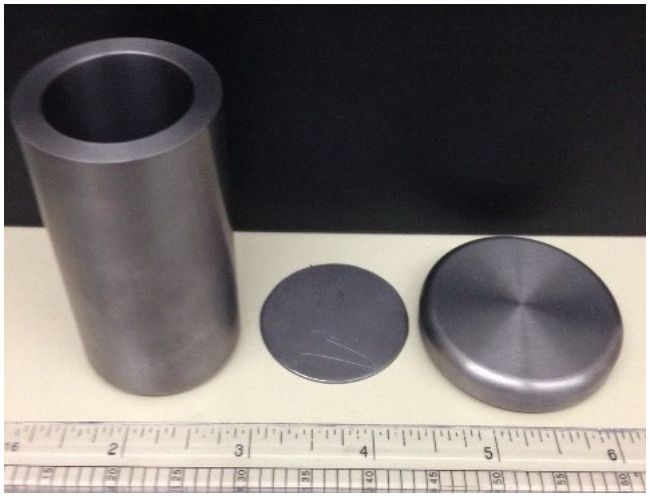

Figure 1. Tantalum Reduction Vessel

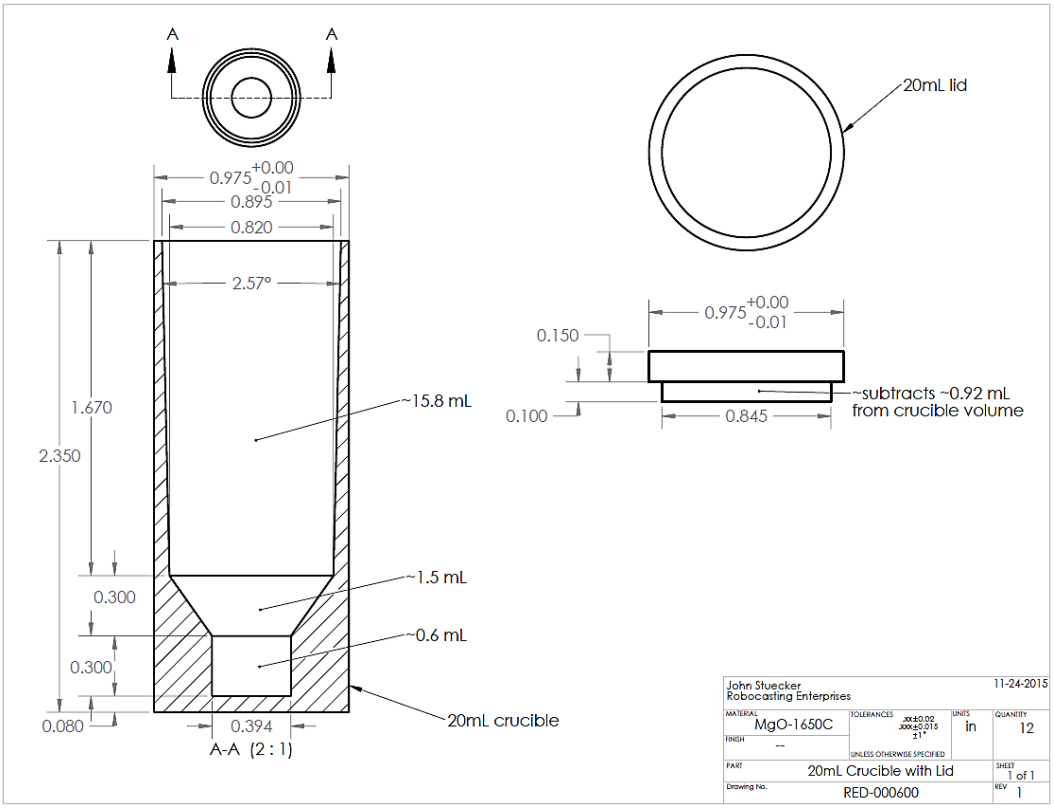

Figure 2. Magnesium Oxide (MgO) Crucible Design

Three U-Zr-Pu buttons[1] and one U-Zr button were produced with this setup. Uranium metal was alloyed with 10 wt% Zr and Pu contents of 10 wt%, 5 wt%, and 2.5 wt%. Additionally, one button of U was alloyed with 10 wt% zirconium, but no Pu, for comparison. The remaining weight fraction of each button was U. The buttons were produced by combining stoichiometric mixtures of UF_4, ZrF_4, and PuO_2, in addition to iodine and approximately 20% molar excess of calcium metal. Iodine was used in combination with the calcium for the additional heat added by it's exothermic reaction with calcium. Before the reactants were loaded, each MgO crucible was heated to 500°C in air to remove residual moisture. The charged crucibles were loaded into the outer vessel and a washer and lid were placed on top. A separate vacuum chamber was used to evacuate the vessel and argon-flush the atmosphere within the vessel three times. After the final cycle, the vessel was transferred into an induction coil within the argon-purged chamber. A pneumatic piston was activated to maintain closure on the lid/vessel interface. The U-Zr-Pu buttons with 5 wt% and 10 wt% plutonium was reduced within the 309 SS vessel. The U-Zr-Pu buttons with 0 wt% and 2.5 wt% plutonium was reduced within the tantalum vessel. The SS susceptor vessel was used in some of this work to determine if it could be reused for multiple iterations. There were no indications that there was a difference in final product between the two vessels. It should be noted that there was greater difficulty removing the crucible contents from the 309 SS vessel and it is recommended that 309 SS vessels be single-use in bomb reduction applications.

[1] The product of this process is typically referred to as a "button," because the metal produced is often in the shape of a button.

3.0 Results

The metallothermic reduction process nominally produces U-Zr-Pu metal and CaF_2 + CaI_2 slag. For this study, the metal yields were in the 60–85% range. The density difference between the metal and the slag provides overall separation during the solidification process; However, the slag is typically adhered to the metal at the interface. Figure 3 shows a button with the slag adhered to the metal. Figure 4 shows the buttons after the slag has been removed. These images were taken through the glove box window.

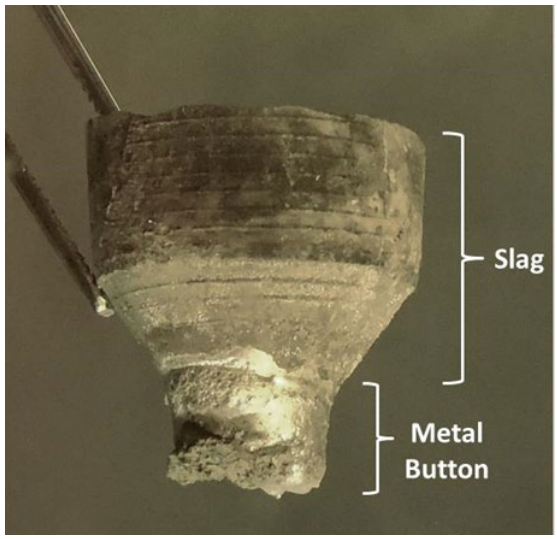

Figure 3. Button with Slag

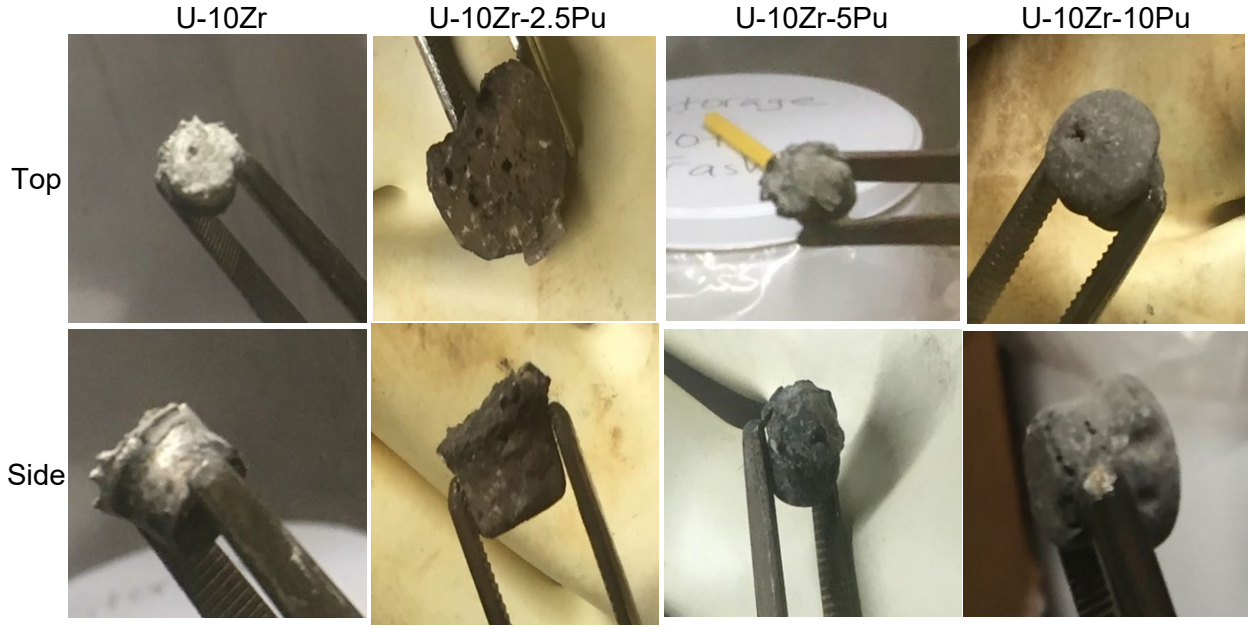

Figure 4. Images of Top (top row) and Side (bottom row) Profiles of Each Button. From left to right: U-10Zr, U-10Zr-2.5Pu, U-10Zr-5Pu, U-10Zr-10Pu.

The mass yields for the U-10Zr, U-10Zr-2.5Pu, U-10Zr-5Pu, and U-10Zr-10Pu reductions were ~78%, ~71%, ~60%, and ~85%, respectively. Variability in the process yield is attributable to variations in homogeneity of the compound, material loss during the loading process, oxidation of the reactants, oxygen content in the atmosphere, and packing efficiency of the reactants. The buttons were sectioned in an air-atmosphere glove box, potted with epoxy, and polished for electron microscopy and powder x-ray diffraction.

3.1 Electron Microscopy

Scanning electron microscopy with EDS was used to analyze local regions of the buttons for inclusions, visible phase formations, and elemental distribution. Figure 5, Figure 6, Figure 9, and Figure 11 are secondary electron images. Figure 7, Figure 8, and Figure 10 are EDS element maps for zirconium, carbon, uranium, plutonium, oxygen (Figure 7 and Figure 8), and silicon (Figure 10).

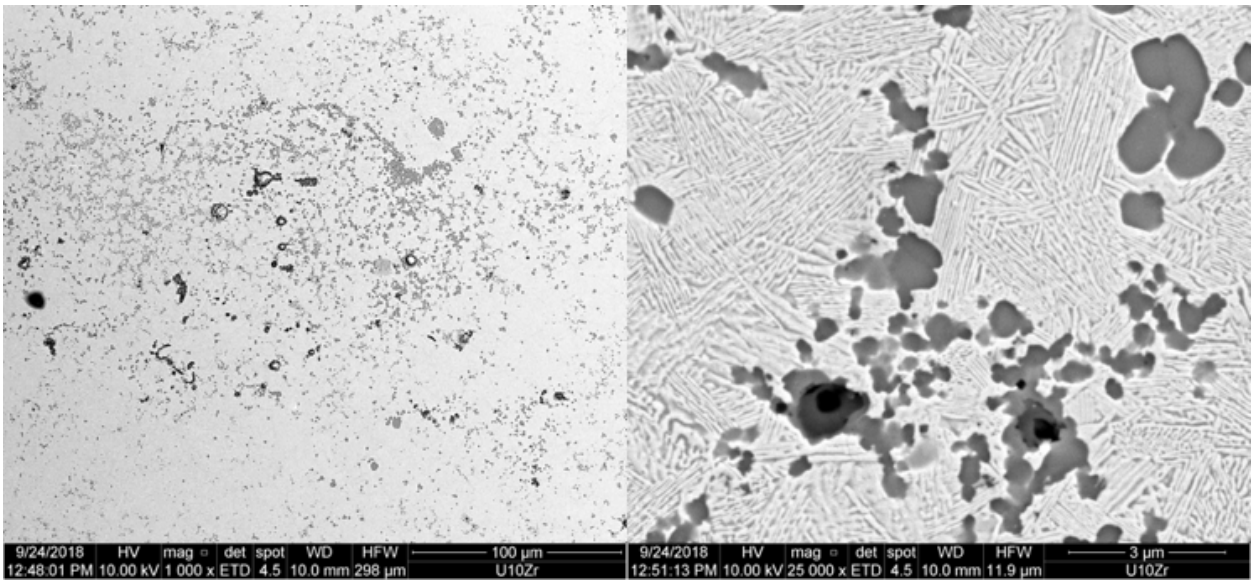

Figure 5. U-10Zr Micrographs (left: 1,000×; right: 25,000×)

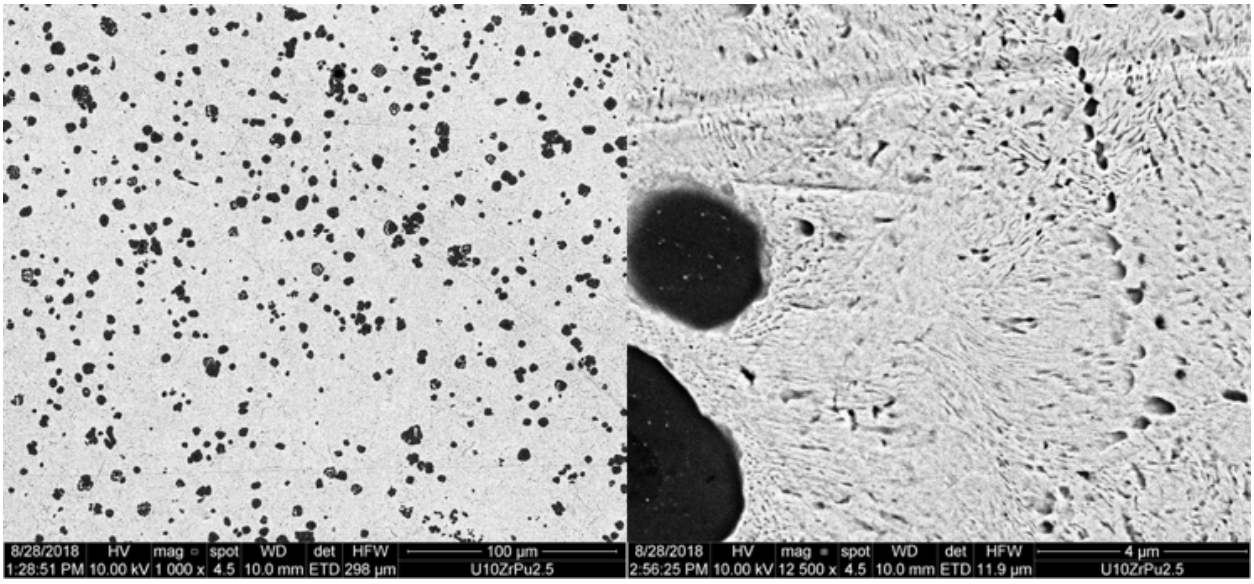

Figure 6. U-10Zr-2.5Pu Micrographs (left: 5,000×; right: 25,000×)

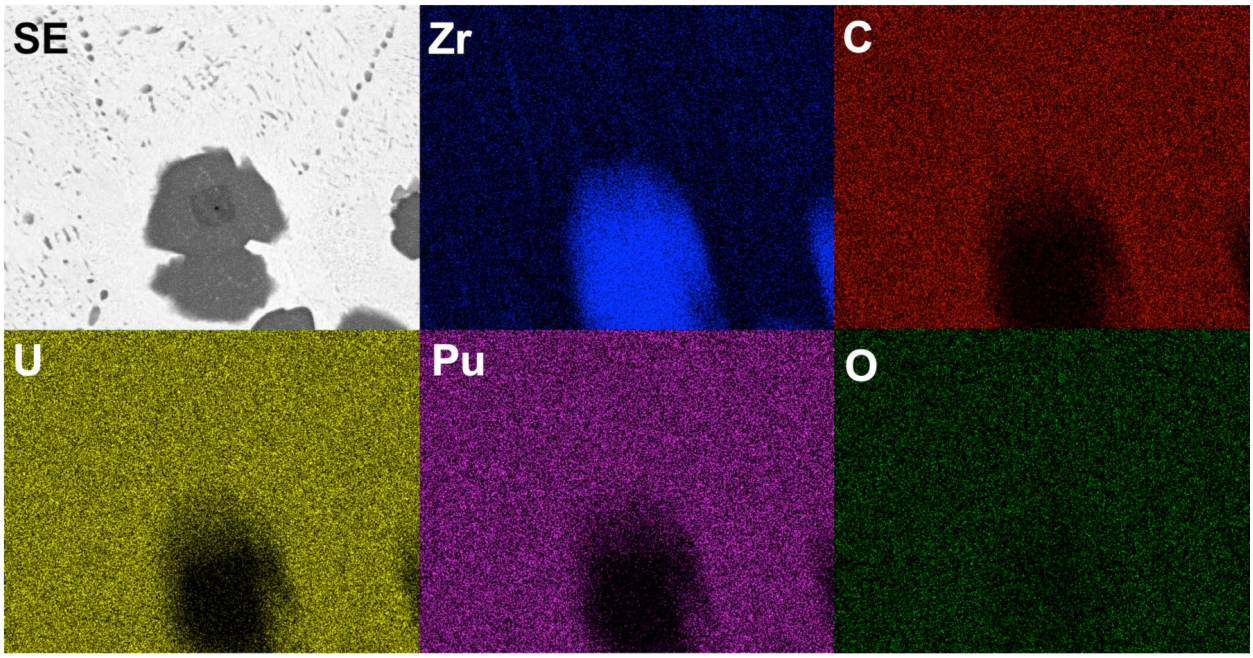

Figure 7. U-10Zr-2.5Pu EDS Element Maps at 20,000× Magnification

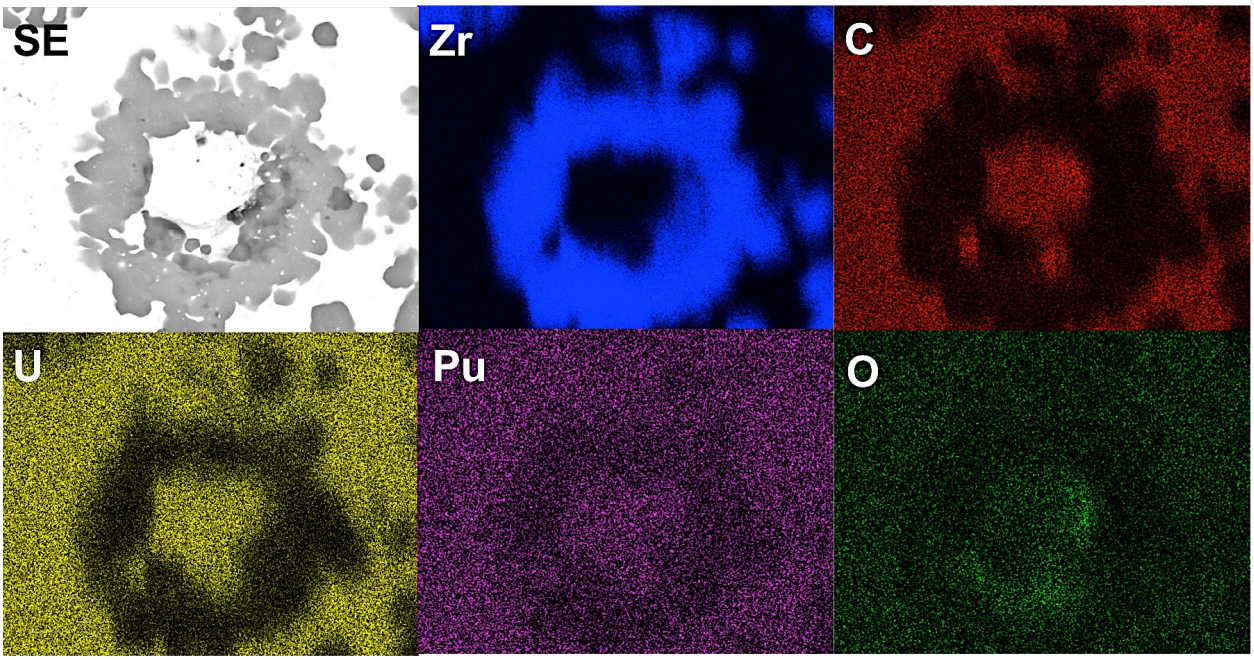

Figure 8. U-10Zr-2.5Pu EDS Element Maps at 10,000× Magnification. SE is secondary electron.

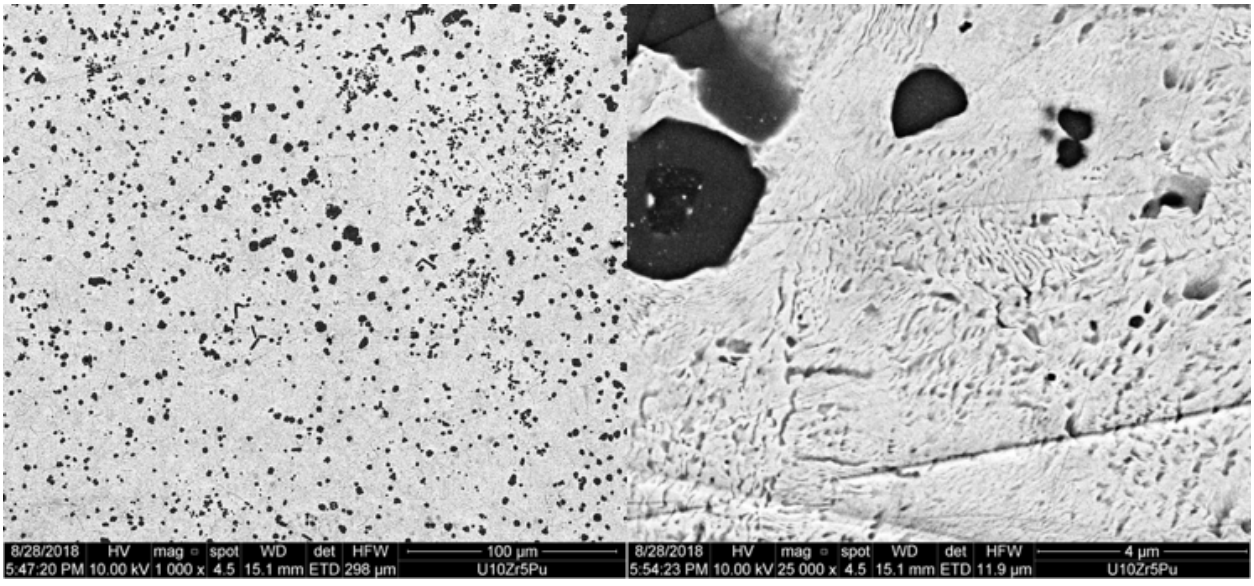

Figure 9. U-10Zr-5Pu Micrographs (left: 1,000×; right: 25,000×)

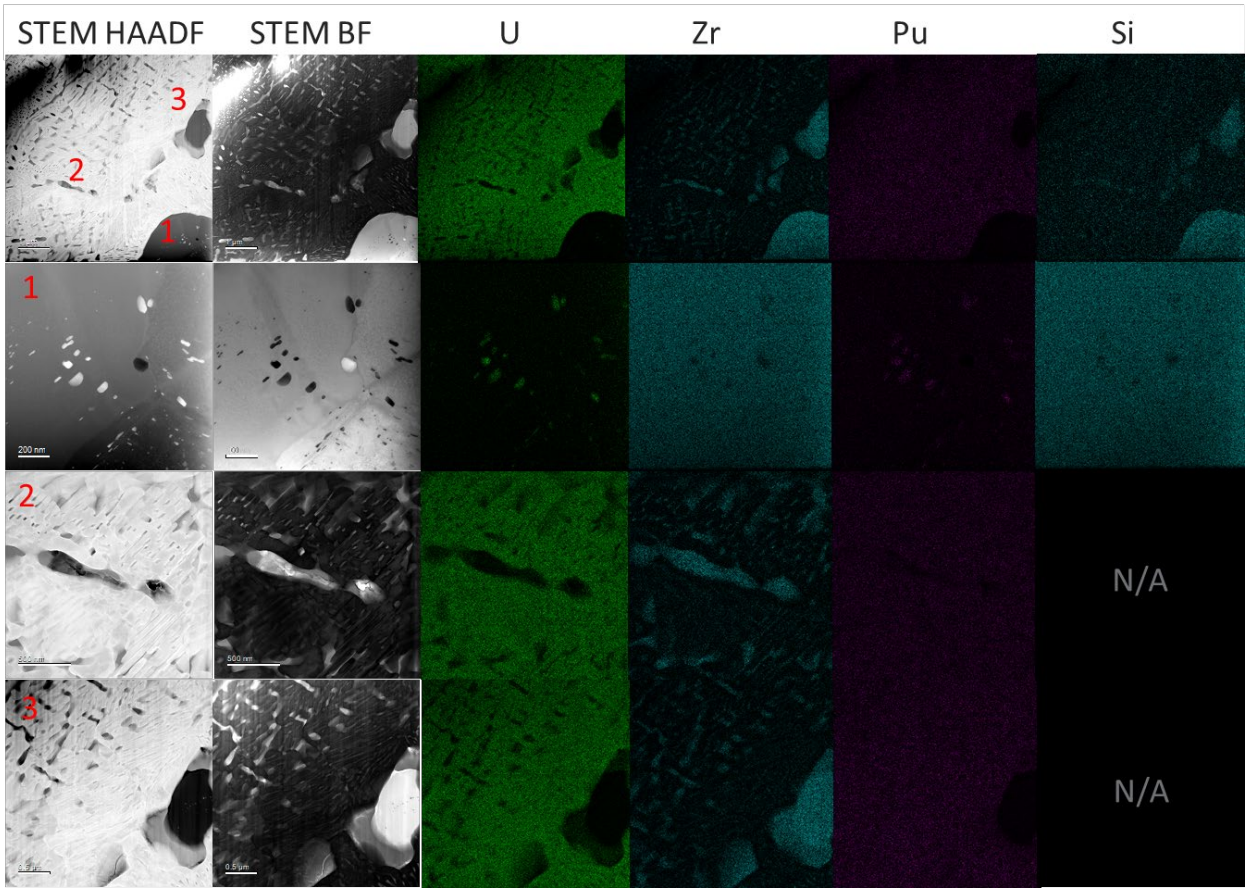

Figure 10. U-10Zr-5Pu EDS Element Maps. Positions marked in the top row correspond to higher-magnification images in subsequent rows. (Top row: 30,000×; second row/Location 1: 150,000×; third row/Location 2: 100,000×; fourth row/Location 3: 60,000×. STEM is scanning transmission electron microscope, HAADF is high-angle annular dark field, BF is bright field).

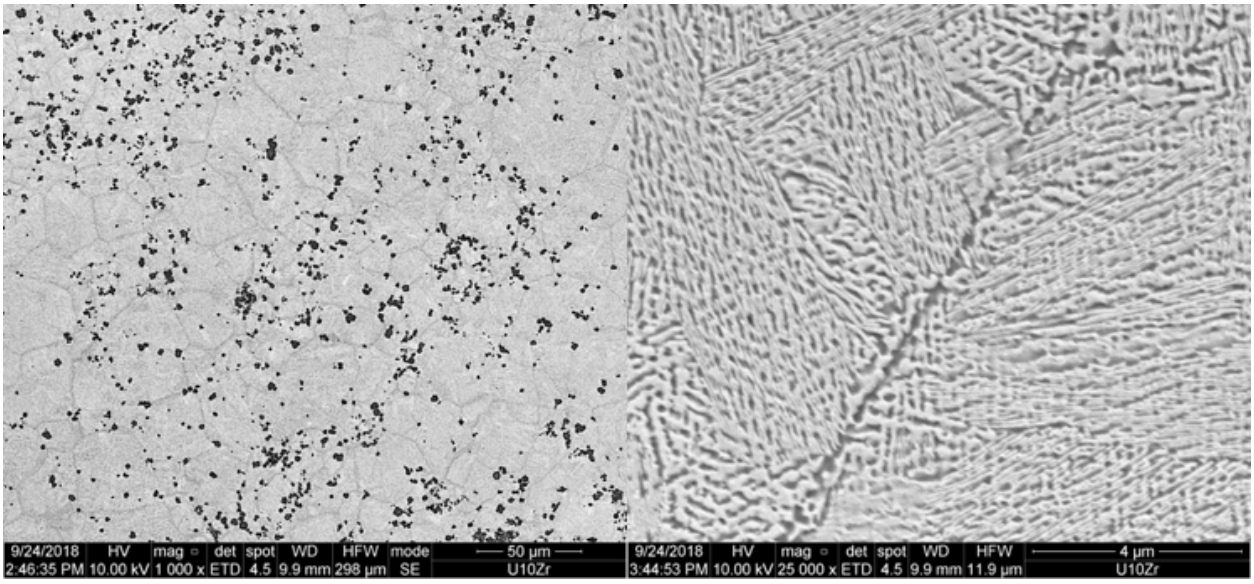

Figure 11. U-10Zr-10Pu Micrographs (left: 1,000×; right: 25,000×)

3.2 Atom Probe Tomography (APT)

A focused ion beam was used to prepare an APT needle at a bulk microstructure/precipitate interface. Figure 12 shows the APT needle location. Figure 13 shows a micrograph and an element map of the needle.

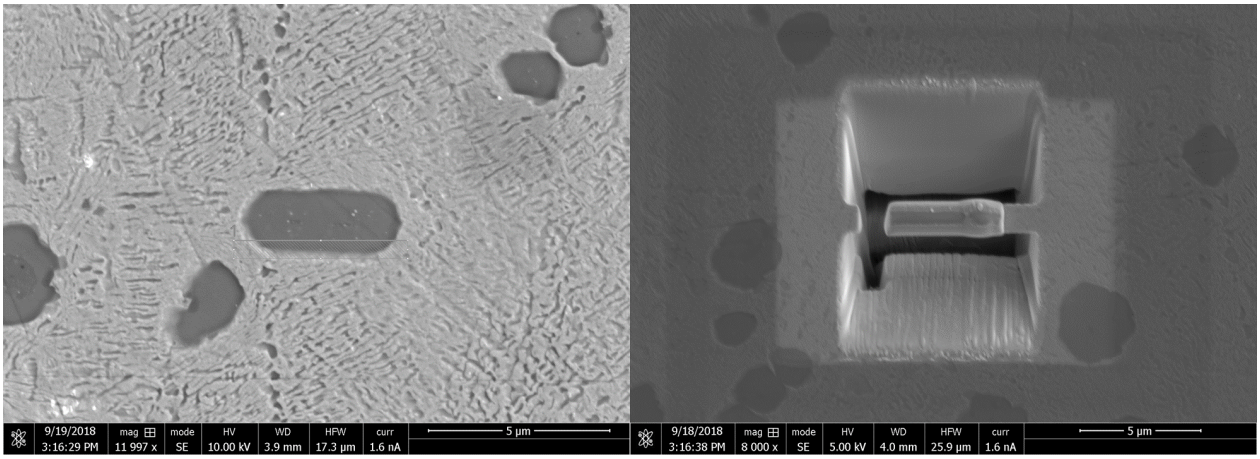

Figure 12. U-10Zr-2.5Pu Micrographs of APT Needle Source Location (left: 12,000×; right: 8,000×). The rounded oblong shape in the left-hand image shows initial FIB work; other darker gray areas are inclusions.

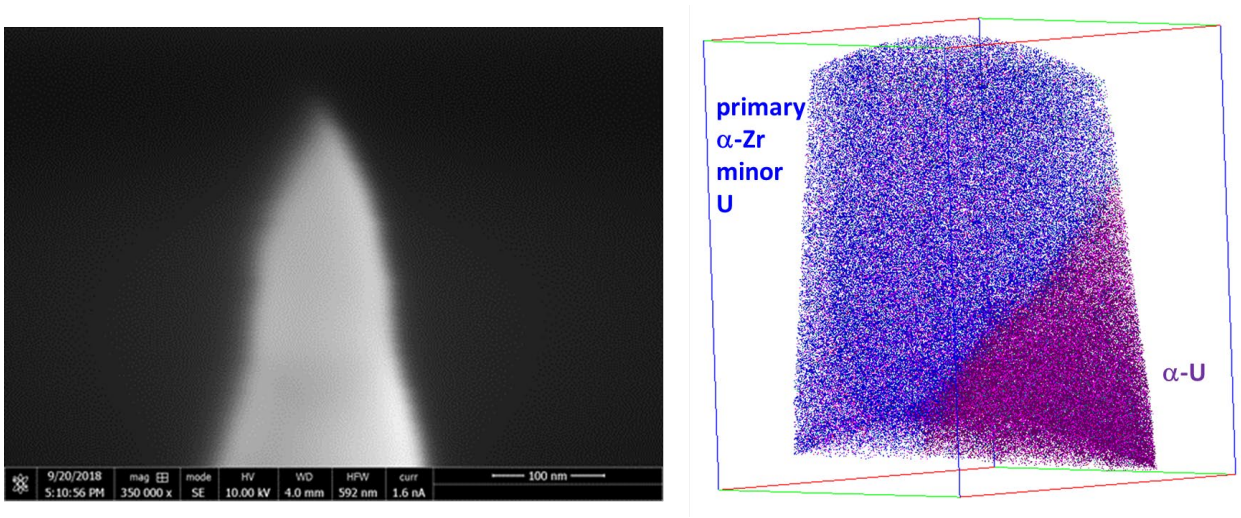

Figure 13. U-10Zr-5Pu Micrograph of APT Needle (left, 350,000×); APT Element Map (right)

3.3 X-Ray Diffraction (XRD)

Room temperature U-Zr alloys with less than approximately 40 wt% zirconium contains primarily alpha phase U and delta phase intermetallic U-Zr. U-10Zr-Pu alloys in the range of 2.5–10 wt% Pu have the potential for a three-phase system: alpha phase uranium, delta phase intermetallic U-Zr, and zeta phase U-Pu (Aitkaliyeva et al. 2016; Capriotti et al. 2017). Figure 14 and Figure 15 show XRD spectra from U-10Zr-2.5Pu and U-10Zr-5Pu, respectively. The results of this XRD analysis were inconclusive in identification of phases other than alpha U, which does not agree with the SEM-EDS, TEM, and APT results. It is unknown what caused this discrepancy and future analysis is warranted.

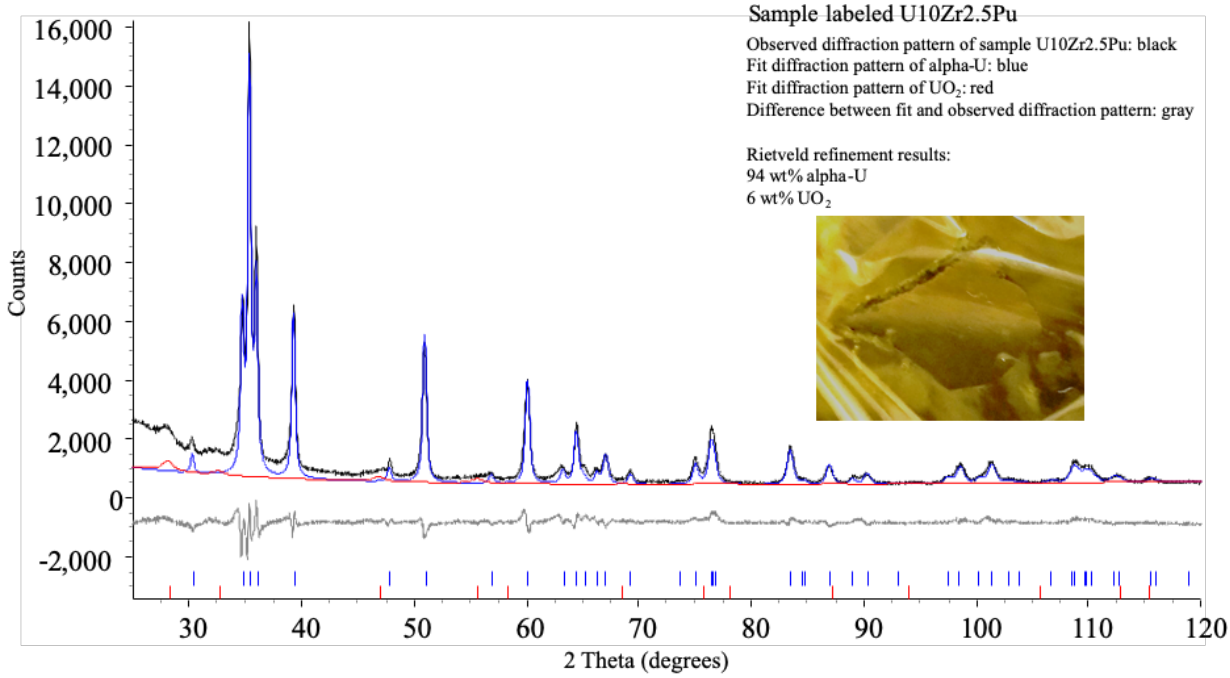

Figure 14. U-10Zr-2.5Pu XRD Spectrum. Inset: photo of specimen.

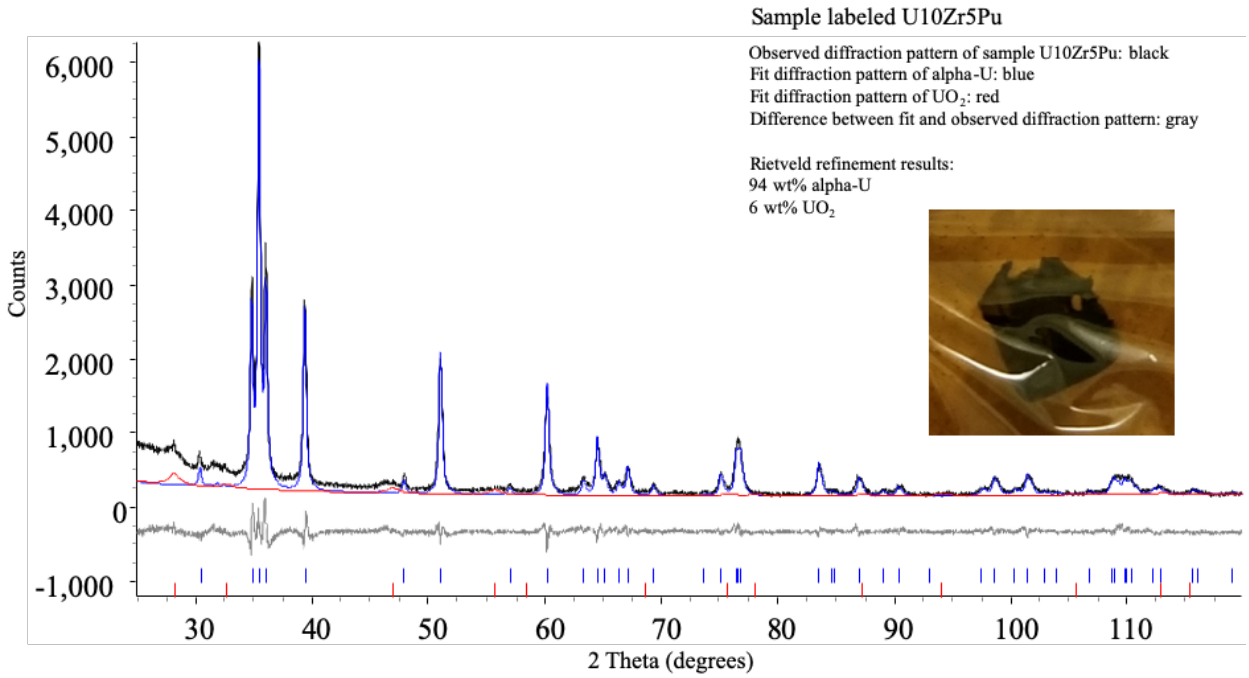

Figure 15. U-10Zr-5Pu XRD Spectrum. Inset: photo of specimen.

4.0 Discussion and Conclusions

The U-10Zr microstructure shown in Figure 5 exhibits alternating lamellar plates typical of alpha phase uranium and delta phase uranium-zirconium. Faint outlines of the prior equiaxed grains of the gamma solid solution phase can be seen. Significant precipitates of impurity-stabilized alpha zirconium and carbides are concentrated at these prior grain boundaries. The U-10Zr microstructural evolution is representative of U-Zr phase transformation of the type $\gamma \rightarrow \beta + UZr_2 \rightarrow \alpha + UZr_2$ (C. Basak et al. 2009; McKeown et al. 2013). This type of microstructural growth is also seen in the uranium-titanium system with $\gamma \rightarrow \beta + U_2Ti \rightarrow \alpha + U_2Ti$ under a slow cooling rate (<2°C/s) (Vander Voort 2000). Considering that the metallothermic reduction process created high temperatures (>1400°C) and occurred in the highly insulating combined refractory vessel/crucible, the microstructure in Figure 5 is consistent with unquenched phase growth.

The microstructural features seen in Figure 6 (U-10Zr-2.5Pu), Figure 9 (U-10Zr-5Pu), and Figure 11 (U-10Zr-10Pu) are similar to those in Figure 5 (U-10Zr). The prior grain boundaries of the gamma solid solution phase in these images are much clearer than those in the U-10Zr micrograph (Figure 5).

The results of these experiments (although not exhaustive in characterization) provide evidence that ternary U-Zr-Pu metallic fuels could potentially be produced using a single calciothermic bomb co-reduction. The benefit of this production method is that it provides a streamlined approach to the formation of a ternary alloy that typically involves multiple processing steps and careful feedstock control. The microstructures indicate that there was extensive phase decomposition and secondary phase impurity precipitation; However, U-Zr-Pu features were identified through the combination of electron microscopy and APT. The results of XRD analysis did not support this conclusion and requires further testing. Future research is warranted to better understand the bulk impurities and phases formed from this production method and studies on the thermomechanical processing protocols are necessary to determine if bomb reduction is a viable option for manufacturing metallic fuels.

5.0 References

Aitkaliyeva, Assel, James W. Madden, Cynthia A. Papesch, and James I. Cole. 2016. "TEM identification of subsurface phases in ternary U–Pu–Zr fuel." *Journal of Nuclear Materials* 473: 75-82. https://doi.org/10.1016/j.jnucmat.2016.02.022. https://www.sciencedirect.com/science/article/pii/S0022311516300538.

Baker, R D, B R Hayward, C Hull, H Raich, and A R Weiss. 1946. *Preparation of Uranium Metal By the Bomb Method.* (United States). https://www.osti.gov/biblio/4324735.

Basak, Chandra Bhanu, N. Prabhu, and Madangopal Krishnan. 2010. "On the formation mechanism of UZr_2 phase." *Intermetallics* 18 (9): 1707-1712. https://doi.org/10.1016/j.intermet.2010.05.006. https://doi.org/10.1016/j.intermet.2010.05.006.

Basak, Chandrabhanu, G. J. Prasad, H. S. Kamath, and N. Prabhu. 2009. "An evaluation of the properties of As-cast U-rich U–Zr alloys." *Journal of Alloys and Compounds* 480 (2): 857-862. https://doi.org/10.1016/j.jallcom.2009.02.077. https://www.sciencedirect.com/science/article/pii/S0925838809003260.

Capriotti, L., S. Brémier, K. Inagaki, P. Pöml, D. Papaioannou, H. Ohta, T. Ogata, and V. V. Rondinella. 2017. "Characterization of metallic fuel for minor actinides transmutation in fast reactor." *Progress in Nuclear Energy* 94: 194-201. https://doi.org/10.1016/j.pnucene.2016.04.004. https://www.sciencedirect.com/science/article/pii/S014919701630083X.

Carmack, W. J., D. L. Porter, Y. I. Chang, S. L. Hayes, M. K. Meyer, D. E. Burkes, C. B. Lee, T. Mizuno, F. Delage, and J. Somers. 2009. "Metallic fuels for advanced reactors." *Journal of Nuclear Materials* 392 (2): 139-150. https://doi.org/10.1016/j.jnucmat.2009.03.007. https://doi.org/10.1016/j.jnucmat.2009.03.007.

Hofman, G. L., L. C. Walters, and T. H. Bauer. 1997. "Metallic fast reactor fuels." *Progress in Nuclear Energy* 31 (1-2): 83-110. https://doi.org/10.1016/0149-1970(96)00005-4. https://doi.org/10.1016/0149-1970(96)00005-4.

McCoy, K. Marie , Zachary Huber, Matthew Athon, Paul MacFarlan, and Curt Lavender. May 2020. *Thermomechanical Processing of Uranium Alloys with 10 and 50 Weight Percent Zirconium.* (Richland, WA, USA: Pacific Northwest National Laboratory). https://www.pnnl.gov/main/publications/external/technical_reports/PNNL-30011.pdf.

McKeown, J. T., S. Irukuvarghula, S. Ahn, M. A. Wall, L. L. Hsiung, S. McDeavitt, and P. E. A. Turchi. 2013. "Coexistence of the α and δ phases in an as-cast uranium-rich U–Zr alloy." *Journal of Nuclear Materials* 436 (1): 100-104. https://doi.org/10.1016/j.jnucmat.2013.01.313. https://www.sciencedirect.com/science/article/pii/S0022311513003541.

Nakamura, Kinya, Takanari Ogata, Masaki Kurata, Takeshi Yokoo, and Michael A. Mignanelli. 2012. "Reactions of Uranium-Plutonium Alloys with Iron." *Journal of Nuclear Science and Technology* 38 (2): 112-119. https://doi.org/10.1080/18811248.2001.9715013. https://doi.org/10.1080/18811248.2001.9715013.

Vander Voort, George F. . 2000. *Metallography: Principles and Practice*. Second ed. Materials Park, OH: ASM International.

Zhang, Yuting, Xin Wang, Gang Zeng, Hui Wang, Jianping Jia, Liusi Sheng, and Pengcheng Zhang. 2016. "Microstructural investigation of as-cast uranium rich U–Zr alloys." *Journal of Nuclear Materials* 471: 59-64. https://doi.org/10.1016/j.jnucmat.2016.01.005. https://doi.org/10.1016/j.jnucmat.2016.01.005.

Pacific Northwest National Laboratory

902 Battelle Boulevard
P.O. Box 999
Richland, WA 99354

1-888-375-PNNL (7665)

www.pnnl.gov